

Reverse-phase chromatography removes double-stranded RNA, fragments, and residual template to decrease immunogenicity and increase cell potency of mRNA and saRNA

Andreja Krušič,^{1,4} Nina Mencin,^{1,4} Marta Leban,¹ Evelin Nett,² Mario Perković,² Ugur Sahin,³ Polona Megušar,¹ Aleš Štrancar,¹ and Rok Sekirnik¹

¹Sartorius BIA Separations d.o.o., Mirce 21, 5270 Ajdovščina, Slovenia; ²TRON – Translational Oncology, Johannes Gutenberg University, Freiligrathstrasse 12, 55131 Mainz, Germany; ³Institute for Immunology, University Medical Center of the Johannes Gutenberg University Mainz, Langenbeck street, 55131 Mainz, Germany

mRNA is produced by *in vitro* transcription reaction, which also leads to formation of immuno-stimulatory impurities, such as double-stranded RNA (dsRNA). dsRNA leads to activation of innate immune response linked to inhibition of protein synthesis. Its removal from mRNA preparations increases efficiency of protein translation. Previous studies identified ion-pair reverse-phase high-performance liquid chromatography as a highly efficient approach for dsRNA removal. Here, we present a comprehensive study of IP-RP LC purification on monolith chromatographic supports for mRNA polishing, demonstrating its ability to remove dsRNA, as well as hybridized RNA fragments and residual DNA template, which are not fully removed by mRNA capture methods. We develop step elution methodology, including at microgram scale with novel spin columns operated by centrifugation. We demonstrate SDVB efficiency across a range of molecular sizes and explore the necessity for temperature control for effective dsRNA removal from self-amplifying RNA. SDVB-purified mRNA and saRNA showed significantly increased transgene expression in cell-based assays and reduced the activation of cell autonomous innate immunity in A549 at early time points. Our findings highlight the importance of IP-RP purification for high-quality mRNA production, while simplifying the technological requirements for its adoption in clinical mRNA and saRNA manufacturing processes.

INTRODUCTION

Increased interest in mRNA as a therapeutic modality stems from its ability to deliver the genetic information of almost any protein *in vitro* or *in vivo*, a tractable production process and promising preclinical and clinical outcomes in areas ranging from vaccines, cancer immunotherapies, protein replacement therapies, regenerative medicine, and cellular reprogramming.¹ Although new production paradigms are emerging (e.g., mRNA production in yeast² or *E. coli*³), mRNA for clinical use is still exclusively produced by *in vitro* transcription (IVT) reaction: an RNA polymerase-catalyzed polycondensation of

NTPs guided by linearized plasmid DNA (pDNA) templates. The production process is relatively short (2–3 days) compared with traditional vaccines (several weeks) and yields between 5 and 15 g/L can easily be obtained.⁴

Phage RNA polymerases, such as T7 RNA polymerase, transcribe the RNA with high fidelity from a linearized pDNA template containing the corresponding promoter; however, multiple impurities are known to form, including short abortive RNA fragments, double-stranded RNA (dsRNA), and full-length anti-sense RNA.⁵ Once transfected into cells, these impurities mimic molecular patterns associated with viral infection triggering an innate immune response, and subsequent protein translation inhibition leads to decreased efficacy of mRNA therapies.^{6,7} Therefore, for efficacious and safe mRNA therapies, it is important to eliminate immuno-stimulatory impurities by ensuring high RNA purity by optimized production processes.

Due to their high physicochemical similarity to single-stranded RNA (ssRNA) like mRNA, dsRNA impurities are not efficiently removed by standard purification methods, including LiCl or alcohol-based precipitation,⁸ size exclusion,⁹ and affinity chromatography on Oligo dT column,¹⁰ which are not able to distinguish between ssRNA and dsRNA (reviewed in Rosa et al.⁴). Anion-exchange (AEX) chromatography for RNA purification has been limited to relatively short sequences (<500 nt).^{8,11} Preparative denaturing polyacrylamide gel electrophoresis (PAGE) is commonly used to purify *in vitro*-transcribed RNA.¹² However, this method is only suitable for short RNAs at small (μg) purification scales, since long RNAs are left untranslatable due to covalent modifications introduced by the denaturants glyoxal and formaldehyde.¹³ Multimodal chromatography (e.g.,

Received 28 June 2024; accepted 17 February 2025;
<https://doi.org/10.1016/j.omtn.2025.102491>.

⁴These authors contributed equally

Correspondence: Rok Sekirnik, Sartorius BIA Separations d.o.o., Mirce 21, 5270 Ajdovščina, Slovenia.

E-mail: rok.sekirnik@biaseparations.com



AEX-hydrogen bonding) achieves partial dsRNA separation from ssRNA, but seems to be limited to short dsRNAs, which are not bound to parent ssRNA.^{14,15} Removal of dsRNA and recovery rates with cellulose chromatography are high (65% and 85%, respectively) at relatively low cost, but challenges in scalability and lot-to-lot reproducibility remain: cellulose chromatography columns are practically challenging to prepare¹⁶; and cellulose particles have been found in mRNA elution fractions, requiring additional filtration steps for removal.¹⁶ RNase III digestion can be used to digest dsRNA fragments,¹⁷ at the cost of introducing an additional enzyme and consequent RNase III-removal purification step but with similar efficacy increase reported as for HPLC purification.¹⁸ RNase III selectivity for dsRNA over secondary ssRNA structures has not yet been thoroughly investigated, potentially posing challenges with RNA sequences with highly structured sections, such as self-amplifying RNA (saRNA). Silica mesoporous particles showed promise in dsRNA removal but are not commercially available, and further research is required to optimize specificity and recovery and minimize potential interference from contaminants.¹⁹

To date, the most effective way to eliminate dsRNA contaminants from long IVT mRNAs is ion-pair reverse-phase high-performance liquid chromatography (IP-RP HPLC),^{16,19–21} which approximately separates according to molecular size, based on RNA hydrophobicity. In the seminal study, removal of dsRNA by IP-RP HPLC from nucleoside-modified mRNA reduced induction of interferons (IFN) and inflammatory cytokines, and translation occurred at much greater levels in primary cells compared with unpurified mRNA.¹⁹ IP-RP HPLC can be performed under non-denaturing conditions (room temperature), partly denaturing, or fully denaturing conditions (60°C and higher; 75°C was shown to fully denature dsRNA into ssRNA).^{20,22} Furthermore, IP-RP HPLC eliminates contaminating RNases.²³

We were intrigued by the potential of IP-RP chromatography to produce mRNA with improved purity, which did not trigger an innate immune response and we wished to address the issues identified by Karikó et al.¹⁹ as limiting factors: scalability, recovery, and the use of acetonitrile (ACN). Other reports agreed that IP-RP is time-consuming, results in recoveries of eluted fragments as low as 50%, and that ACN toxicity could preclude its use in clinical manufacturing.⁷

Previously reported IP-RP mRNA work was performed with non-porous particle chromatographic supports, which may have contributed to the limitations observed in (1) scalability, since extremely low porosity of the material generates high back-pressures for chromatographic experiments, reducing working flow rates or requiring extremely high pressures for operation which are not practical at pilot or production scales; and (2) recovery, due to low binding capacity resulting from relatively low surface area available for binding of analytes.^{24,25}

CIM monolith chromatography media was designed with highly interconnected networks of large channels (2–6 µm) without dead-end pores, enabling convective mass transport of analytes, resulting

in capacity and resolution that are not compromised by the slow diffusion constants of large mRNA. Multiple publications reported high recovery of mRNA purifications with monolith chromatographic supports where porous particle media either showed low recovery (anion exchange/multimodal chromatography^{14,15}) or flow-rate dependent loss of binding capacity.²⁶ Hence, we postulated that use of monoliths could alleviate the recovery, scalability, and speed constraints of IP-RP identified by others,^{16,19,27} and we set out to build on proof-of-concept studies by Gagnon who demonstrated separation of DNA, dsRNA, and ssRNA synthetic standards by size on poly(styrene-co-divinylbenzene) (SDVB) monoliths.²⁸ We wished to explore the versatility of available SDVB monolith formats, from chromatographic skid-operated large-scale columns to centrifuge-operated spin columns. Our goal was to facilitate the efficient removal of immunogenic RNA contaminants for both large-scale (multi-mg) and small-scale (µg) mRNA preparations, as well as related modalities, including significantly longer sequences such as saRNA. We also examined the subsequent impact of this purification on transgene expression, viability and interferon response.

RESULTS

Ion-pair reverse-phase chromatographic purification of mRNA in linear ascending ACN gradient

Optimization of mRNA polishing by IP-RP chromatography was based on previously published analytical separation on SDVB monolith^{28,29} and preceding studies on particle-based chromatography.²¹ Initially, we screened the effect of ion pairing reagent triethylammonium acetate (TEAA) concentration on dynamic binding capacity (DBC₁₀), of SDVB for mRNA. The inflexion point of the curve was 50 mM, resulting in an optimal ratio between binding capacity and reagent consumption (Figure S1); further increase in TEAA to 100–300 mM resulted in comparatively small further increase in DBC₁₀ (10%–40%), therefore we proceeded with 50 mM in all subsequent studies. DBC did not vary between flow rates of 0.5–5 CV/min, confirming that DBC of IP-RP chromatography on SDVB monolith is flow-rate independent (Figure S2). Following previous IP-RP publications,²³ 7.5% ACN was used for loading to enable retention of the mRNA. A shallow gradient (95 CV) to 18% ACN resulted in a broad elution peak spanning ~40 CV (elution completed at 13% ACN), after which the column was stripped in 18% ACN and sanitized with 75% ACN (Figure 1A).

Fragment Analyzer identified short RNA sequences (200–800 nt), significantly below the target molecular weight of eGFP mRNA, in fraction 1 eluting at approximately 9.3% ACN (17% MPB; Figure 1B). Fraction 2 contained lower molecular weight RNA sequences as well as full-length mRNA. The first two elution fractions were positive on J2 dot blot (Figure 1C), indicating the presence of dsRNA. Full-length mRNA, which was J2-negative, eluted in fractions 3–11. Strip fraction, which represented <1% of total peak area, exhibited a strong J2 response, suggesting a high relative abundance of dsRNA sequences or longer dsRNA stretches (e.g., 3' extended transcripts; Figure 1C).

To establish whether short RNA fragments in early SDVB elution were IVT-derived, we prepared ARCA-capped eGFP mRNA, which

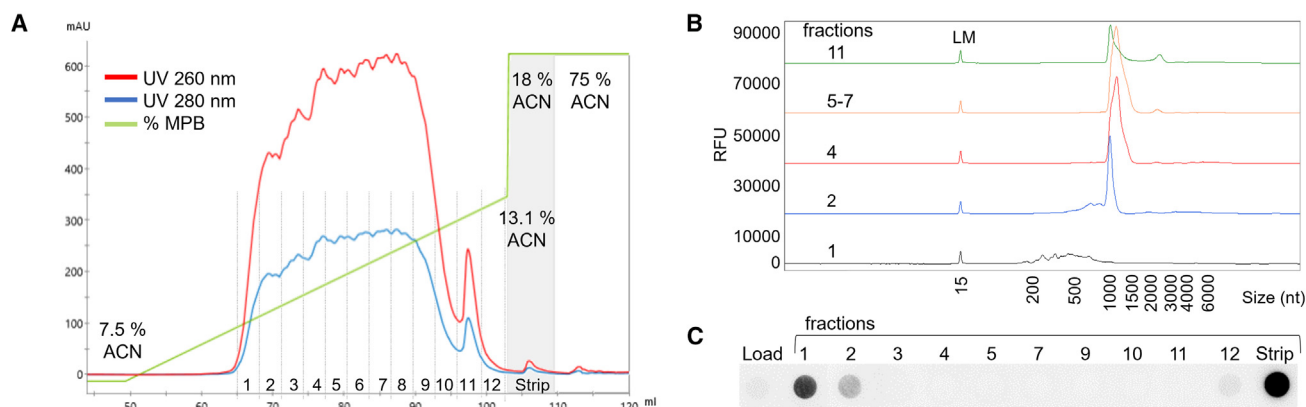


Figure 1. Ion-pair reverse-phase polishing of mRNA on CIMmultus SDVB with linear gradient removes dsRNA and truncated RNA

(A) A mass of 0.5 mg of Oligo dT pre-purified mRNA (eGFP) was loaded onto 1 mL CIMmultus SDVB column at room temperature and eluted in linear gradient from 7.5% to 18% ACN over 95 CV at 1 CV/min. (B) Fragment Analyzer electropherograms of selected fractions show lower molecular weight (MW) impurities eluting in fractions 1 and 2, with higher MW impurities observable in fractions 5–7 and significant in fraction 11. LM: Low molecular weight marker. (C) Elution fractions were analyzed on J2 dot blot, which confirmed the presence of dsRNA sub-populations in fractions 1, 2, 12, and strip.

was first purified with Oligo dT and then subjected to the same elution gradient on SDVB, with the ascending part of the elution peak (up to 10.5% ACN) fractionated in 0.5 CV intervals (data not shown). All collected fractions were analyzed for molecular size, 5' capping using a capping efficiency assay, and presence of polyA tail using an analytical CIMac Oligo dT assay (Figure 2). Consistent with the initial experiment on uncapped mRNA, early elution (fractions 1–6) contained RNA sequences of 200–750 nt length with no detectable full-length mRNA (Figure 2A); these fractions were 75%–85% capped (Figure 2B), but only 20%–25% bound to CIMac Oligo dT, indicating that the majority lacks polyA tail and that they likely originate from premature termination during the transcription process (Figure 2C: elution). Mid-elution (fractions 7–15) contained an increasing percentage of full-length mRNA signal and increasing binding to CIMac Oligo dT column alongside lower molecular weight (MW) impurities, while capping was still >75%. Full-length mRNA signal continued to increase in main elution (fractions 16–21), which predominantly contained higher MW impurities (fraction 19 had 87% mRNA in Oligo dT elution). Overall, analytical Oligo dT column recovered 85% of the starting material (SDVB Load), suggesting that at least this amount of IVT product contained intact polyA tail (Figures 2C and S3). To verify if SDVB purification leads to fragmentation of mRNA, we reinjected the main, fragment-free SDVB elution peak, following an identical purification SDVB protocol. Elution fractions, including the earliest UV signal increase, contained no detectable fragments or J2 dot blot signal (Figure S4). Linear gradient experiments thus demonstrated that mRNA devoid of fragments and dsRNA can be obtained with >76% recovery at room temperature.

IP-RP mRNA purification with step elution

Linear gradient elution strategy requires fractionation and purity analysis before fraction pooling, which can slow production processes due to the need for in-process analytical gating. We therefore inves-

tigated a step elution strategy for IP-RP purification of mRNA to speed up and simplify in-process control (IPC) analytics and avoid the need for pooling decisions.

Increased mRNA mass loading on SDVB led to earlier onset of elution (increasing loading from 50 µg to 150 µg, ACN required for mRNA elution decreased from 11.4% to 9.4%; Figure S5). We therefore optimized mRNA step elution protocol at room temperature based on estimates of ACN concentration for desired peak elution from the linear gradient experiment, at a constant load challenge (0.6 mg/mL or ~86% DBC), on 0.2-mL and 1-mL columns (Figure 3A). Experiments on an 8-mL CIMmultus SDVB column performed under the same conditions resulted in a consistent recovery of >85% (Figure 3B): material was loaded in 7.5% ACN (0% MPB), washed with 8.5% ACN (10% MPB), and eluted with 11.7% ACN (40% MPB), followed by a final strip with 18% ACN (100% MPB). Consistent with the analysis of linear gradient elution fractions, the wash step (fraction 1) exhibited truncated RNA sequences on Fragment Analyzer, and a weak J2 dot blot signal, indicating the presence of short RNA chains containing dsRNA structures. The elution step contained the desired MW peak as the major product, with short dsRNA impurities below the detection limit of respective analytical methods (fractions 2 and 3). The strip step resulted in a peak with lower UV intensity, containing higher MW species (>2000 nt) and a very strong J2 dot blot signal, suggesting that these likely correspond to incompletely denatured multimeric eGFP species, or 3' extended transcripts (although at room temperature the possibility of mRNA multimers cannot be excluded).

This step method was then translated to larger column volume (80 mL CIMmultus SDVB column, Figure 3C). Minor modification of steps was required for scale-up with an additional 9.6% ACN wash step (20% MPB), and process recovery was 69%. Variation is

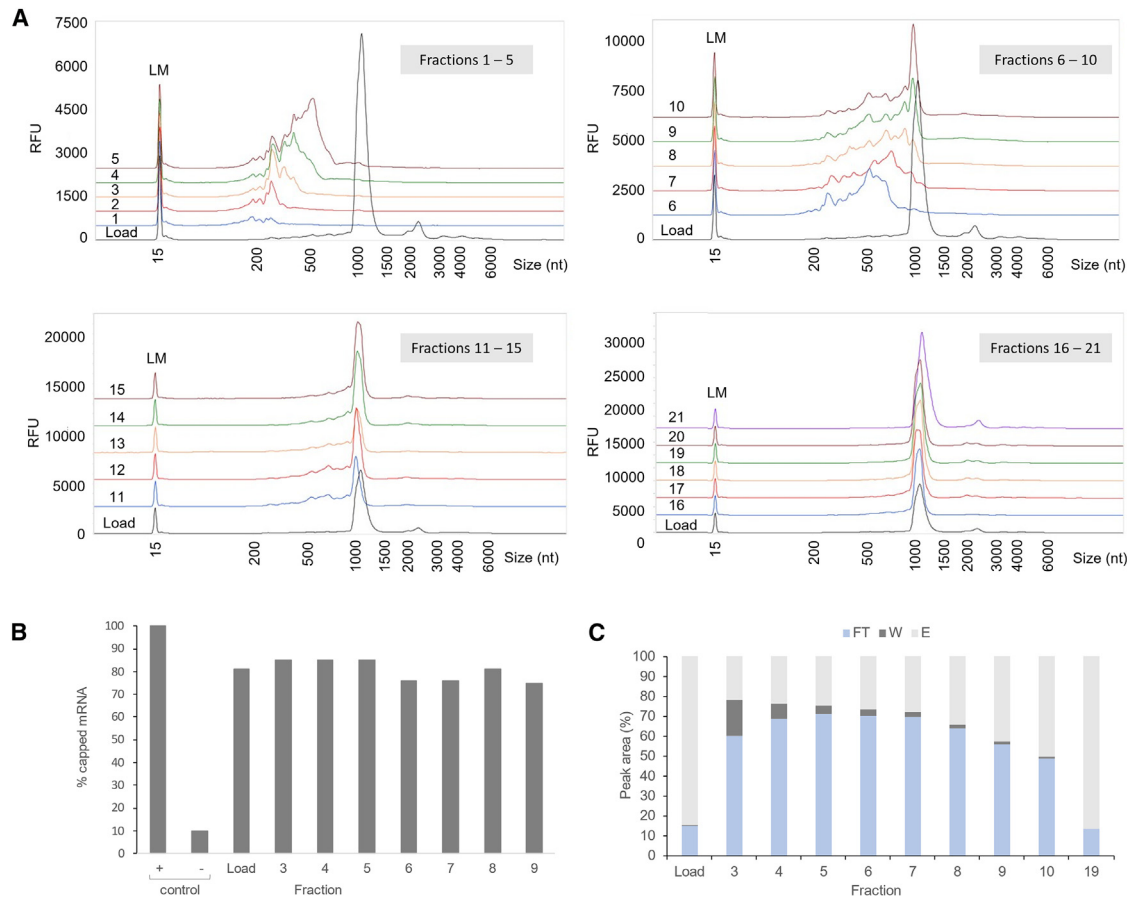


Figure 2. Analytical characterization of RNA fractions collected from SDVB linear gradient purification

A mass of 0.5 mg of ARCA-capped mRNA eGFP, pre-purified with CIM Oligo dT, was loaded onto CIM SDVB column at room temperature and eluted in a linear gradient (from 7.5% to 18% ACN over 95 CV) at 1 CV/min. The first 10 mL of elution peak was collected in 20 fractions (1-20), and the remaining 30 mL was collected as one fraction (21). (A) Fragment Analyzer results show RNA size distribution in fractionated elution peak. LM: molecular weight marker. (B) Capping efficiency analysis of selected elution fractions. (C) CIMac Oligo dT chromatographic analysis indicates % polyadenylation of elution fractions. Relative amounts of unbound, non-specifically bound, and bound RNA are presented in the bar chart, from integration of CIMac Oligo dT flow-through (FT), wash (W), and elution (E) peaks, respectively.

likely due to minor differences in chromatographic equipment specifications, mobile phase batch-to-batch variability, or CIP strategy applied at 80-mL scale (NaOH-based CIP procedure was applied to 80-mL column as opposed to 75% ACN to reduce ACN consumption, see [materials and methods](#)). Elution fraction purity remained consistent at this scale: wash (fraction 1) and strip exhibited a positive J2 dot blot signal, while elution (fractions 3 and 4) did not ([Figure 3C iii](#)). Residual pDNA template was identified in the early and strip fractions, but not in elution fraction, by agarose gel electrophoresis (AGE) ([Figure 3C iv](#)) and CIMac pDNA residual template quantification ([Figure 3C v](#)). pDNA detected in early SDVB fractions had the predicted molecular size by AGE but did not migrate with electrophoretic mobility of linearized pDNA standard on native PAGE, while the pDNA from strip fraction did ([Figure 3C](#)). DNA electrophoretic bands were absent in SDVB step elution fractions of mRNA that had been treated with DNase I prior to IP-RP separation ([Figure S7](#)). In absence of DNase I digestion, proteinase K treatment did not affect

the amount of residual pDNA template in Oligo dT elution ([Figure S8](#)).

Downscaling of the mRNA purification for laboratory applications using spin columns

With verified step elution conditions, it is possible to perform purification without online UV absorbance measurements and, by inference, without chromatographic equipment. Spin columns, widely used in kit format for isolation of pDNA and mRNA from crude mixtures at laboratory scale, could in principle also be used to remove dsRNA. We tested step elution conditions optimized for eGFP mRNA construct on prototype CIM SDVB spin columns (0.1 mL bed volume) using a benchtop centrifuge. Satisfyingly, applying identical mobile phase compositions to centrifuge-operated spin columns resulted in a purity profile highly comparable to purifications executed on chromatography

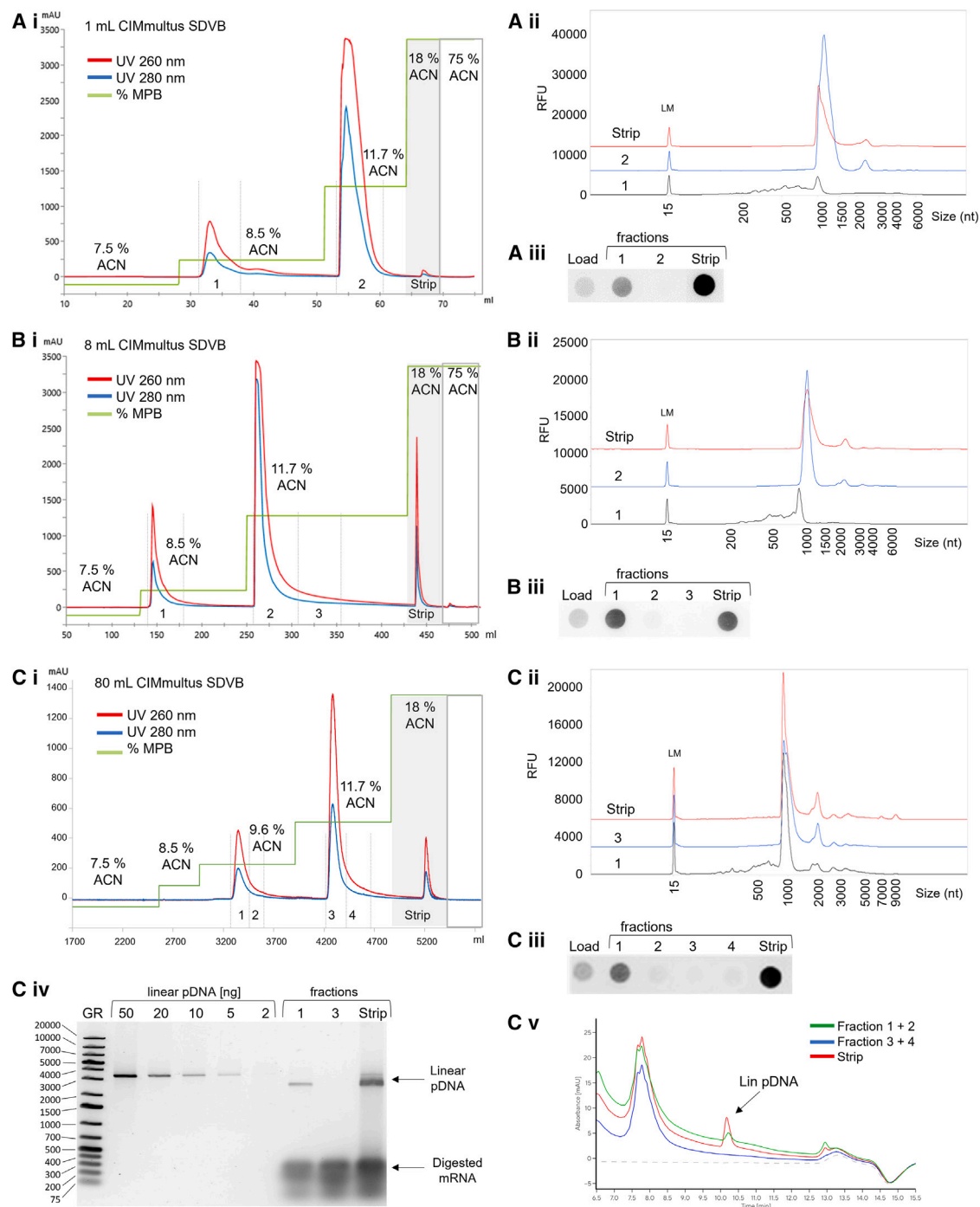


Figure 3. Ion-pair reverse-phase polishing of mRNA with CIMmultus SDVB operated with step elution removes dsRNA, truncated RNA, and residual pDNA template at least to 80-mL column scale

Purification of (A.i) 0.6 mg and (B.i) 4.8 mg of Oligo dT-prepurified mRNA eGFP on 1 mL and 8 mL CIMmultus SDVB column, respectively, at room temperature and at 1 CV/min. Step elutions of 8.5% ACN, 11.7% ACN, and 18% ACN were applied. (A.ii and B.ii) Fragment Analyzer results of corresponding fractions. (A.iii and B.iii) J2 dot blot confirmed clearance of truncated sequences and dsRNA species in main mRNA fractions ("2"). (C.i) Scale-up preparative chromatogram of Oligo dT-prepurified mRNA (48 mg) on 80 mL CIMmultus SDVB column at room temperature and at 2 CV/min operated with Hipersep Flowdrive Pilot HPLC chromatography system. Step elutions were fractionated in five fractions (1–4 and strip). (C.ii) Fragment Analyzer and (C.iii) J2 dot blot analytics of collected fractions. (C.iv) AGE residual DNA template analysis and (C.v) CIMac pDNA quantification of residual DNA template in collected fractions.

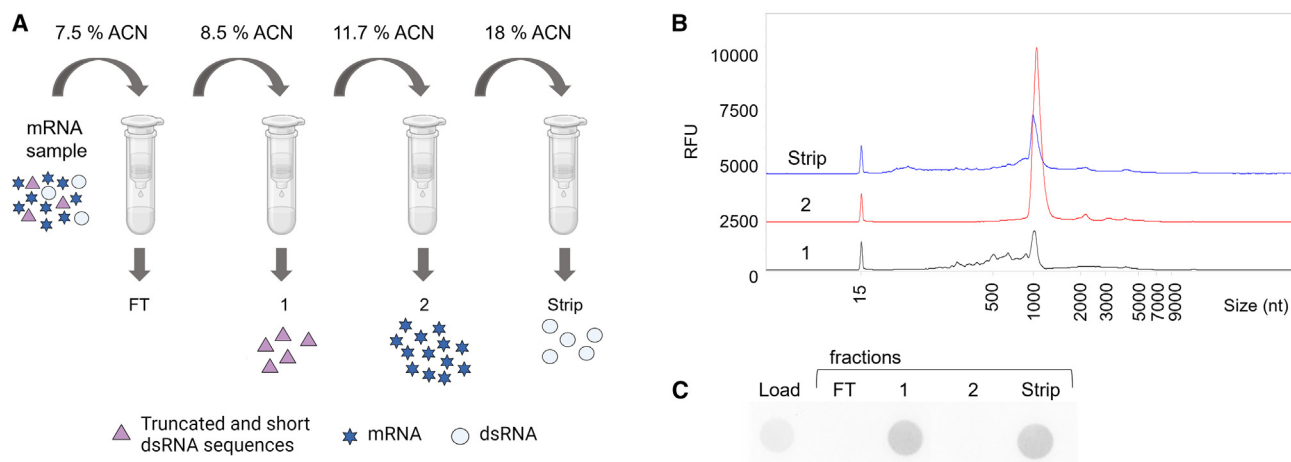


Figure 4. mRNA polishing to remove dsRNA performed with CIM SDVB spin (0.1 mL) column in a benchtop centrifuge

(A) A mass of 95 μ g of Oligo dT-prepurified mRNA eGFP was diluted 10 times in loading buffer containing 7.5% ACN and applied onto a CIM SDVB spin (0.1 mL) column. Wash with 8.5% ACN eluted truncated species (fraction 1), elution with 11.7% ACN yielded full-length RNA (fraction 2) and strip with 18% ACN eluted dsRNA (strip). Recovery of mRNA in fraction 2 was 77%. (B) Fragment Analyzer of load, fractions 1, 2, and strip. (C) J2 dot blot of collected fractions.

skids: wash step (fraction 1) was J2-positive and contained RNA fragments, elution (fraction 2) did not exhibit a detectable J2 signal or fragments and strip fraction was strongly positive on J2 dot blot (Figure 4).

SDVB purification of saRNA

To confirm the generality of IP-RP approach with SDVB monoliths, purification was verified on a significantly longer saRNA construct mCHIK(S27) (9787 nt). Prior to SDVB experiments, mCHIK(S27) saRNA was purified from IVT with CIM Swiper achieving clearance of IVT components, such as NTPs, DNA template, and proteins.¹⁵

Initial screening of elution conditions in 5% MPB (cca 0.5% ACN) increments from 7.5% to 18% ACN was performed on a CIM SDVB 0.2-mL column (loading 0.5 mg saRNA per mL of chromatographic support) to guide optimization toward a three-step method. It is notable that removal of dsRNA was not achieved at room temperature and required elevated temperatures of at least 38°C (applied to the column and mobile phases) regardless of whether the purification was performed in linear gradient or as step elution (Figure S9). Nonetheless, even at elevated temperatures, step elution achieved only partial size-based separation of low molecular weight impurities (fragments), without sufficient improvement in purity profile (Figures S10A and S10B), although residual DNA template and dsRNA were removed (Figures S10C and S10D). Reversion to a linear gradient elution (from 7.5% to 18% ACN) at 40 or 50°C achieved comparable dsRNA clearance, but far superior size-based separation, resulting in successful isolation of >90% pure elution fractions (Figure 5).

In vitro testing of SDVB-purified mRNA and saRNA

Our next aim was to evaluate the physiological impact of removing product-related impurities in cellular models, and we hypothesized

that performing SDVB purification to eliminate impurities would increase transcriptional efficiency by reducing immunogenicity of mRNA and saRNA. To assess the functionality of mRNA purified either with (1) Oligo dT (“w/o SDVB”), (2) Oligo dT plus linear gradient SDVB (“linear-SDVB”), or (3) Oligo dT plus step gradient SDVB (“step-SDVB”), samples were tested in BHK-21 cells. BHK-21 is a cell line deficient in type I IFN activation^{30,31} and allows determination of mRNA or saRNA expression and replication independent from its activity to trigger innate immunity. GFP was used as a transgene encoded on mRNA. After liposome-mediated transfection of the three differently purified mRNA samples, neither a difference in total GFP expression (Figure 6A) nor in relative viability (Figure 6B) was observed. Similarly, transfection of saRNA, encoding for the transgene firefly luciferase, purified with Swiper (“w/o SDVB”) or with Swiper and linear-SDVB (“+ SDVB”), as shown in Figure 5 (fractions 6–7), resulted in comparable firefly luciferase levels with any of the three tested doses (Figures 6C and S11A). None of the samples had a significant cytotoxic effect on BHK-21 cells (Figure 6D). These results indicate that the additional purification step does not impair the functionality of mRNA or saRNA, while the percentage of dsRNA present in the saRNA is not sufficient to make any difference in protein expression.

Next, mRNA and saRNA were separately transfected into A549 cells, a cell line known to express IFNs in response to viral infection, which consequently limits RNA expression.³¹ Purification of Oligo dT mRNA with linear SDVB gradient, as well as step-SDVB, resulted in about 3-fold higher GFP expression (Figure 7A). Furthermore, significantly smaller decrease in viability (Figure 7B) as well as lower IFN β release (Figure 7C) in response to mRNA purified with both SDVB strategies was observed. Similarly, SDVB-purified saRNA resulted in significantly greater transgene expression levels, particularly pronounced at 24 h after transfection (Figure S11B). Total transgene

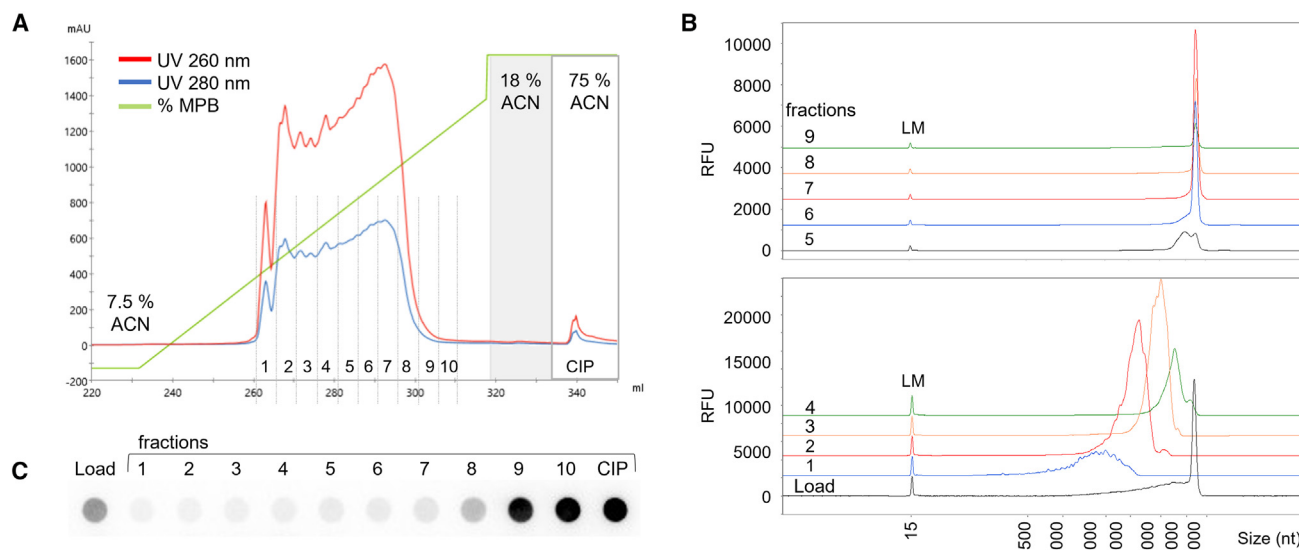


Figure 5. Linear gradient SDVB purification of long saRNA construct on CIMmultus SDVB column

(A) A mass of 1.5 mg of saRNA mCHIK(S27) (pre-purified with CIM Swiper multimodal column) was loaded onto a 4-mL SDVB column at 50°C and eluted in linear gradient from 7.5% to 18% ACN over 25 CV at 1 CV/min. (B) Fragment Analyzer electropherograms of sample load and elution fractions 1–9. (C) J2 dot blot analysis of collected fractions.

expression after 72 h was increased by up to 17-fold, and subsequently a 16-fold lower dose of SDVB-purified saRNA provided 6-fold higher luciferase expression than saRNA that was not SDVB-purified: AUC_{6–72h} 1.29E7 relative light units (RLU) for 10 ng + SDVB vs. 0.23E7 RLU for 160 ng w/o SDVB (Figure 7D). SDVB purification apparently reduced RNA toxicity about 5%, although the differences were not significant (Figure 7E). IFN β levels in the supernatant 6 h after transfection were dose-dependent and decreased by SDVB purification; however, at 24 h, IFN β levels reached comparable or even higher levels in cells treated with saRNA + SDVB than w/o SDVB (Figure 7F).

After confirming the superior performance of SDVB-purified saRNA with reduced impurities in immortalized cells, our next objective was to verify these findings in peripheral blood mononuclear cells (PBMCs). Given that PBMCs contain various human immune cell types, they represent a more physiologically relevant model for RNA treatment. While transgene expression of saRNA w/o SDVB was close to the assay limit of detection, saRNA + SDVB reached significantly higher transgene expression levels (Figure S11C). Total transgene expression was increased with all three tested doses by up to 26-fold (Figure 8A). Furthermore, relative viability was slightly higher with saRNA + SDVB (Figure 8B). Levels of IFN β secreted by PBMCs in response to saRNA were comparable irrespective of SDVB treatment (Figure 8C).

DISCUSSION

In the present study, we optimized mRNA polishing by IP-RP chromatography for scalable mRNA purification. Ion pairing reagent (TEAA) was initially optimized for optimal ratio of reagent

consumption and binding capacity; the latter was shown to be flow-rate independent between 0.5 and 5 CV/min, consistent with prior reports of flow-rate independent monolith properties. Furthermore, consistent steepness of the breakthrough curves indicated that mass transfer remained convective even at higher flow rates.

Linear gradient elution experiments revealed the presence of short RNA fragments in early SDVB elution, indicating that short RNA sequences were either not removed during the capture step (Oligo dT) or were created during sample processing by IP-RP. To exclude the latter, we subjected the main elution peak, which was shown to be fragment-free, to a repeated SDVB purification protocol, which resulted in no detectable fragments or J2 dot blot signal (Figure S4), confirming that short RNA fragments were derived from preceding steps (either Oligo dT purification or IVT). Hence, use of affinity chromatography alone for purification of mRNA produced by IVT reactions was confirmed as insufficient to eliminate immune-stimulatory impurities. Although general base-catalyzed random RNA hydrolysis through 2'OH as described before³² cannot be excluded, the results are consistent with presence of abortive transcripts and truncated sequences that are formed during the initiation of transcription, when T7 polymerase randomly aborts RNA synthesis.³³ These aberrant RNA fragments can randomly prime to complementary RNA and initiate RNA-dependent RNA polymerase activity, which leads to formation of dsRNA contaminants of various lengths.^{34–36} Furthermore, the results suggest that, at least in part, the fragments, which may form dsRNA, interact with complementary RNA sequences and co-purify through Oligo dT with full-length

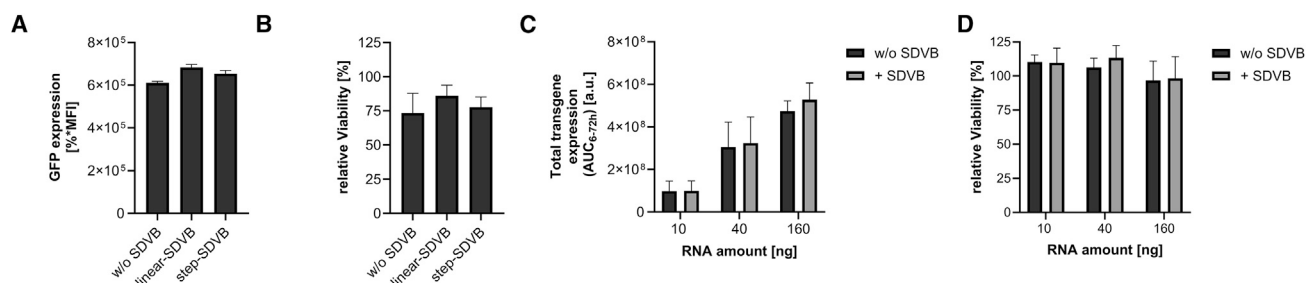


Figure 6. Purification of mRNA and saRNA with CIM SDVB does not compromise functionality in immuno-incompetent BHK-21 cells

(A) A mass of 100 ng mRNA purified with Oligo dT ("w/o SDVB") or Oligo dT + SDVB with linear gradient elution strategy ("linear-SDVB") or Oligo dT + SDVB with step elution strategy ("step-SDVB") was transfected into BHK-21 cells. After 24 h, GFP expression was measured by flow cytometry. The mean fluorescence intensity was multiplied with the percentage of GFP expressing cells to receive the total GFP expression levels. (B) Relative viability of cells was assessed by measuring viability after 48 h and normalized to the mock control. (C) BHK-21 cells were lipofected with the indicated doses of either Swiper ("w/o SDVB") or Swiper and SDVB-purified saRNA (" +SDVB"). Luciferase expression was measured 6, 24, 48, and 72 h after transfection. Area under the curve (AUC) was calculated to determine the total luciferase expression. (D) Viability was measured 48 h after transfection and normalized to the mock control. Mean and standard error of the mean (SEM) of three independent experiments, each performed in technical triplicates, are shown.

mRNA; it is unclear how these dsRNA structures interact with mRNA that binds to Oligo dT; under IP-RP conditions, interaction with the parent mRNA is weakened and short, dsRNA-forming fragments are separated under acetonitrile gradient, while dsRNA is not efficiently destabilized by ACN at room temperature, and remains in double-stranded form, resulting in intense J2 dot blot signal of early SDVB fractions (Figure 1).

Strong J2 dot blot signal was also observed in the peak tail and in the strip fraction. It is assumed that strip fractions contain longer dsRNA molecules (extended duplexes) that are formed from 3' extension of the mRNA product, which folds back and anneals to the complementary sequences on the same RNA molecule or anneals to a second RNA molecule.³⁷ These structures have greater hydrophobic surface, bind more strongly to reverse-phase support, and therefore require higher organic solvent concentration for elution compared with less hydrophobic full-length mRNA.¹⁹

Successful development of a step elution strategy at room temperature for IP-RP chromatographic purification of mRNA greatly simplifies the technological requirements for manufacturing processes, by reducing in-process control (IPC) analytics and avoiding the need for pooling decisions. Step elution was shown to be applicable on a wide range of purification scales and technologies, from 0.1 mL bed volume CIM SDVB spin columns operated with benchtop centrifuges, up to large-scale purification of 48 mg of Oligo dT-prepurified mRNA eGFP on an 80 mL CIMmultus SDVB column, requiring only minor modifications of mobile phase compositions. A known challenge is dependence of elution conditions on mass loading (increased mass loadings lead to earlier onset of elution), requiring lower % ACN for elution of short fragments (Figure S5). It is therefore important to maintain constant loading in step elution methods to reach optimum recovery of purified RNA, and this should particularly be borne in mind when translating to larger scales.

It has been reported that if the linearized pDNA template was not digested with DNase I post-IVT, mRNA capture methods do not completely remove the pDNA template (which was only reduced to 0.1%–0.4%³⁸) and it had been suggested that IP-RP achieves pDNA clearance comparable to DNase I.³⁸ We confirmed that SDVB can remove residual pDNA template from mRNA so that no residual pDNA is detected in the main elution fraction of SDVB, but surprisingly found residual pDNA both in early (low ACN) and late (high ACN) fractions (Figure 3). Elution of pDNA template at a later retention time compared to mRNA was expected based on previous reports,^{28,29} but elution of pDNA before the main mRNA was surprising. pDNA detected in early SDVB fractions had the predicted molecular size by AGE, but did not migrate with electrophoretic mobility of linear pDNA standard on native PAGE, while the pDNA from strip fraction did (Figure S6), suggesting that early SDVB fraction contains pDNA complexed with a non-DNA species, either RNA-DNA hybrid or an RNA-DNA-T7 transcription bubble.³⁶ In absence of DNase I digestion, proteinase K treatment did not affect the amount of residual pDNA template in Oligo dT elution (Figure S8), suggesting that residual pDNA is not complexed to mRNA via T7 or other IVT proteins, but thus more likely interacts directly with mRNA.

Verification of an IP-RP purification approach with SDVB monoliths on a significantly longer (9787 nt) saRNA construct mCHIK(S27) revealed two important aspects of general applicability: (1) linear gradient elution provided superior size-based separation, which is required for much larger RNA molecules containing relatively more high-molecular weight contaminants; (2) room temperature was not sufficient to remove dsRNA contaminants from full-length saRNA. To investigate if an increase in column temperature improved chromatographic separation of saRNA, heating between 25°C and 50°C was applied (to the column and mobile phases). In order to minimize thermal hydrolysis

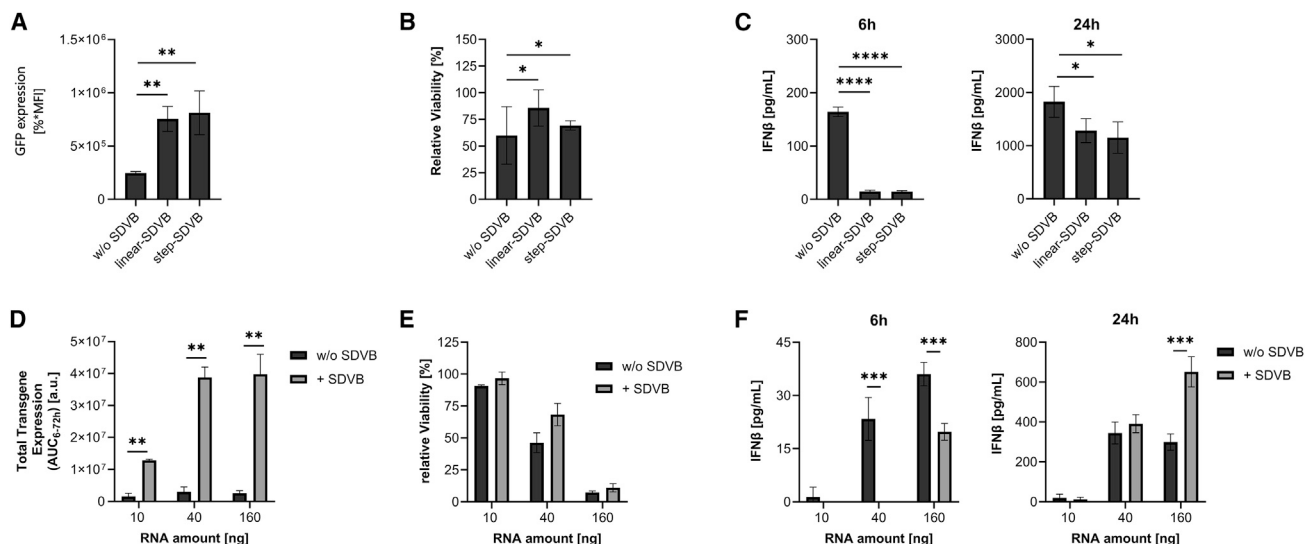


Figure 7. SDVB purification of mRNA and saRNA improves transgene expression in A549 cells, where IFN β response limits expression

(A) A549 cells were lipofected with 100 ng of mRNA purified with Oligo dT ("w/o SDVB") or Oligo dT plus SDVB with linear gradient elution strategy ("linear-SDVB") or Oligo dT plus step elution strategy ("step-SDVB"). Twenty-four hours after transfection, GFP expression was detected by flow cytometry. (B) Viability of cells was detected 48 h after lipofection and normalized to untreated cells. (C) IFN β release into the supernatant was quantified by ELISA 6 and 24 h after transfection. (D) 10, 40, or 160 ng of saRNA without ("w/o SDVB") or with (" + SDVB") SDVB purification was transfected into A549 cells. Luciferase expression was measured at 6, 24, 48, and 72 h after transfection and area under the curve was calculated to assess total transgene expression. (E) After 48 h, ATP levels were quantified and normalized to the levels of untreated cells to determine relative viability. (F) 6 and 24 h after lipofection, IFN β levels in the supernatant were quantified by ELISA. Mean and standard error of the mean of three independent experiments, each done in technical triplicates, are shown. Statistical differences were calculated using two-sided unpaired t tests with p values lower than 0.05 considered as significant and classified into *: $p < 0.05$; **: $p < 0.01$; ***: $p < 0.001$; ****: $p < 0.0001$.

of RNA, the lowest possible temperature was sought, and the flow rate throughout the purification process was increased to 5 CV/min to reduce the time that saRNA was exposed to elevated temperature. We observed a gradual decrease in dsRNA content in main elution fraction (Figure S9F, "fraction 2") as the temperature increased, with a minimum temperature required for efficient dsRNA removal of 38°C. Comparable dsRNA removal with CIM SDVB at 38°C was achieved regardless of whether purification was performed in linear gradient or step elution (Figure S9), while fragment removal was superior with linear gradient compared with step (Figures 5 and S10).

Similarly, for mRNA, further increasing the temperature of SDVB purification to 50°C led to a decreased J2 signal of early fractions (and increased recovery of J2-negative mRNA), confirming that dsRNA species can be partly denatured from mRNA prior to chromatographic separation (Figure S12), which increased recovery of pure mRNA by up to 20%. Increasing temperature is thus a possible general approach to increase recovery of dsRNA-free mRNA/saRNA, although the relative increase in recovery must be assessed against the practical challenges of heating the chromatographic system and possible sample degradation.

In vitro, we could validate that purification improvements translated to an enhanced performance of SDVB-purified RNAs; however, exposing RNA to an additional purification step with

increased temperatures might also impact its functionality. This might be especially important for saRNA, which incorporates stem-loop structures that are required for replication. BHK-21 cells are deficient in type I IFN activation,^{30,31} which is crucial for activation of cell autonomous innate immunity. This defense system involves a variety of sensors and mechanisms that detect the presence of pathogens but also gets activated by IVT RNA.⁵ We observed comparable transgene expression levels from RNA produced without or with SDVB purification in BHK-21 cells, which indicated that the additional purification step does not impair the functionality of mRNA and saRNA (Figures 6A and 6C). Immunocompetent A549 cells and PBMCs, which are potent in sensing and reacting to non-self RNA structures,³⁹ demonstrated that eliminating product-related impurities reduces the immunogenicity of the RNA sample and allows more efficient mRNA and saRNA expression (Figures 7A, 7D, and 8A). This is of particular interest because saRNA without sophisticated purification had been shown to be able to give protection in mice against viral infection equivalent to mRNA vaccines but at much lower doses.⁴⁰ SDVB purification may allow further reduction of the protective dose. Increased transgene expression from SDVB-purified saRNA is in accordance with findings that reducing innate immune response activation by using modified nucleotides increases the potency of saRNA.^{41,42} Increased IFN β levels at later time points in A549 cells and in PBMCs in response to saRNA may be explained by greater saRNA replication where dsRNA occurs

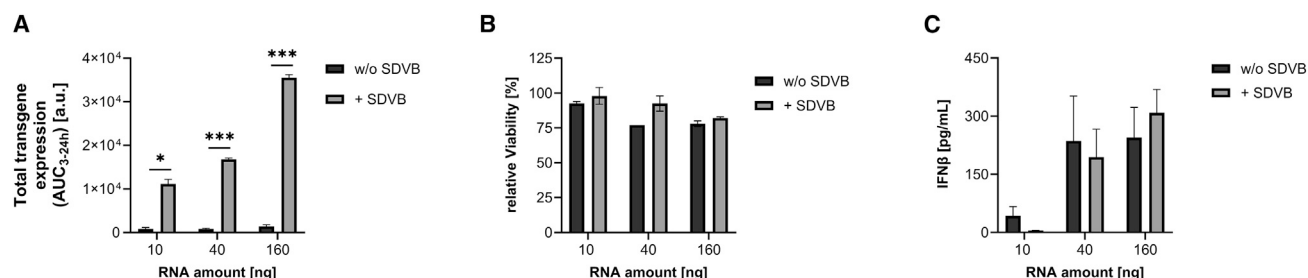


Figure 8. CIM SDVB purification of saRNA allows transgene expression in PBMCs

saRNA mCHIK(S27) without ("w/o SDVB") or with (" + SDVB") SDVB purification was lipofected at 10, 40, and 160 ng into PBMCs. Luciferase expression was measured at 3, 6, 9, and 24 h after transfection. (A) Area under the curve was calculated to assess total transgene expression. (B) Viability was measured 24 h after lipofection and normalized to the untreated cells to assess relative viability. (C) Secreted IFN β levels in the supernatant were quantified by ELISA 6 h after transfection. Error bars depict standard error of the mean from three independent experiments with triplicates each. Statistical differences were calculated using two-sided unpaired t tests with *p* values lower than 0.05 considered as significant and classified into *: *p* < 0.05; **: *p* < 0.01; ***: *p* < 0.001; ****: *p* < 0.0001.

as an intermediate replication product and is being sensed by cellular antiviral machinery.

Conclusions

We have developed a scalable purification of mRNA and saRNA based on IP-RP chromatography with CIM monolith chromatographic support (SDVB). We show that early SDVB fractions consistently contain short RNA fragments, which were derived from the Oligo dT purification step or preceding steps, rather than being generated during the IP-RP polishing step. Longer dsRNA sequences, likely corresponding to 3' extensions and full complements, elute in late fractions. Both early and late fractions contain dsRNA species, while main elution fractions contain full-length, J2 dot-blot negative mRNA/saRNA.

We show that SDVB removes residual pDNA template, thus obviating the need for DNase treatment. Future work can investigate the different populations of residual DNA template separated by SDVB into early and late fractions.

We implemented step elution strategy for IP-RP purification of mRNA to speed up and simplify the downstream purification process and simplify IPC analytics. Percentage of acetonitrile required to maximize removal efficiency for RNA fragments, dsRNA, and DNA template varied based on RNA length and RNA mass loading. Therefore, method optimization may be warranted to maximize purity and yield for different RNA constructs to deliver the full benefit of step elution approach. SDVB-purified mRNA and saRNA demonstrated enhanced performance in cell-based assays, with reduced initial immunogenicity of IVT RNA and increased transgene expression in immunocompetent cells. Importantly, we demonstrated for the first time that RNA can be polished to remove immunogenic impurities with a simple, centrifuge-operated spin column approach, similar to extraction kits commonly used for extraction of pDNA or RNA, and accessible to most RNA/DNA laboratories. This has the potential to increase the quality of RNA drug substance used for early preclinical studies, thereby potentially reducing the attrition of RNA-based therapies that may have been discarded due to under-

appreciated effect of purity profile on immunogenicity and efficacy, which could not be mitigated by traditional laboratory RNA purification techniques used to produce them.

MATERIALS AND METHODS

Chemicals and reagents

All CIMmultus (Convective Interaction Media) chromatography columns (Oligo dT and SDVB) had 2- μ m channel diameter and were from Sartorius BIA Separations. Buffer solutions were freshly prepared with double-distilled water (ddH₂O) from Adrona water purification system and analytical grade reagents. Acetonitrile (ACN), agarose, ammonium acetate, skim milk powder (non-fat dried milk), sodium chloride (NaCl), triethylammonium acetate (TEAA), Trizma base and boric acid were from Sigma-Aldrich. Hydrochloric acid and sodium hydroxide were from Honeywell, Tween 20 was from VWR, MgCl₂ was from Invitrogen, and Kompleksal III (EDTA-Na₂x2H₂O) was from Kemika. Mobile phases for scale-up experiments on 80 mL CIMmultus SDVB (50 mM TEAA, 7.5% acetonitrile, pH 7.0 and 50 mM TEAA, 18% acetonitrile, pH 7.0) were from ADS Biotec. Vivacon 500 and Vivaspin 2, 30000 MWCO, Hydrosart were from Sartorius. All IVT reagents (RNase Inhibitor Murine, NTP mix, Pyrophosphatase, T7 RNA Polymerase, Anti-Reverse Cap Analog [ARCA]) were from MEBEP Bio Science, CleanCap AU was from TriLink BioTechnologies. Restriction enzyme SapI and DNase I with reaction buffer were from NEB, RNase A was from Monarch, RNA 5' Polyphosphatase with RNA 5' Polyphosphatase Reaction Buffer were from Lucigen, Terminator 5'-Phosphate-Dependent Exonuclease and Terminator Reaction Buffer A were from Biosearch Technologies. For J2 dot blot experiment, Biotyne Pre-Cut Nylon membrane and western blotting filter paper were from Thermo Fisher Scientific, Magi2 dsRNA standard (1,000 base pairs [bp]) was from RNA Greentech, anti-dsRNA primary antibody J2 was from Jena Bioscience, secondary antibody Peroxidase AffiniPure Goat Anti-Mouse IgG (H + L) was from Jackson ImmunoResearch, and WesternBright ECL was from Advantia. For electrophoresis experiments, 6% Novex TBE Gels, denaturing 6% Novex TBE-Urea Gels, Novex Hi-Density TBE Sample Buffer (5X), Novex TBE-Urea Sample Buffer (2X), SYBR Gold Nucleic Acid Gel

Stain, and GeneRuler 1 kb Plus DNA Ladder were from Invitrogen (Thermo Fisher Scientific).

BHK-21 cells were from ATCC (CCL10) and A549 cells from Abcam (ab255450). All media (Eagle's minimum essential medium, F-12K Nutrient Mixture-Kaighn's RPMI Modification medium) as well as non-essential amino acids and sodium pyruvate were from HiMedia, fetal calf serum from Bio&Sell, plasma-derived human serum from OneLambda. Nunc MicroWell 96 Well plates, RNase-free tubes and Lipofectamine MessengerMax were from Thermo Scientific, OptiMEM, and phosphate-buffered saline from Gibco. The luminescence-based assays Bright Glo and CellTiter Glo were both from Promega, the Spark multimode microplate reader used to measure luminescence from Tecan. LumiKine Xpress hIFN- β 2.0 was from InvivoGen.

E. coli cell pellet containing plasmid encoding mRNA eGFP (size 995 nt) was provided by Biomay AG and plasmid for saRNA mCHIK(S27) encoding chikungunya replicase and firefly luciferase (size 9787 nt) was provided by TRON (Mainz, Germany).

mRNA synthesis and capture purification

Isolation of pDNA encoding mRNA eGFP from *E. coli* paste, plasmid purification and linearization was performed as described previously.⁴³

The same pDNA purification protocol was used for plasmid pCHIK(S27), which was subsequently linearized with SapI enzyme. IVT protocols used to produce mRNA/saRNA used in the study are listed in Table S1. The IVT reactions were quenched with 30 mM EDTA (final concentration) and immediately purified. Where applicable, DNase digestion of pDNA template was performed after IVT by incubating the mixture with DNase I in 1X reaction buffer (1 U of enzyme per μ g pDNA) for 15 min at 37°C. Purification of mRNA by hybridization-affinity chromatography on CIMmultus Oligo dT column was performed as described elsewhere.⁴³ saRNA was purified either with CIM Swiper (Sartorius BIA Separations, not commercially available) as previously described¹⁵ or with CIMmultus Oligo dT as follows: sample was first diluted 5-fold in 50 mM Na-phosphate, pH 7.4 and loaded on the column by in-line dilution (dilution ratio 1:1) in 50 mM Na-phosphate, 0.75 M NaCl, pH 7.4, washed with 50 mM Na-phosphate, 0.15 mM NaCl, pH 7.4, and eluted in ddH₂O. After purification, the RNA concentration was determined using NanoDrop One (Thermo Fisher Scientific).

IP-RP chromatographic purification of mRNA and saRNA with CIM SDVB

Small-scale chromatographic experiments on CIM SDVB 0.2 mL disc were performed on a PATfix analytical system (Sartorius BIA Separations), experiments on CIMmultus SDVB 1-mL and 8-mL column were performed on ÄKTA pure 150M (Cytiva) and scale-up experiment on CIMmultus SDVB 80 mL column was performed on Hipersep Flowdrive Pilot HPLC system (Sartorius). UV absorbance was monitored at 260 nm and 280 nm. Dynamic binding capacity

(DBC₁₀) was calculated from the breakthrough curve at 10% maximal UV signal at 1 mg/mL. PATfix software (Sartorius BIA Separations), UNICORN software (Cytiva), and Hipersep Flowdrive SC software (Sartorius) were used for instrument control, data acquisition, and data analysis.

For each purification experiment with CIM SDVB, the mRNA or saRNA sample was diluted 10-fold in loading buffer 50 mM TEAA, 7.5% ACN, pH 7.0 (mobile phase A, MPA), prior to processing on SDVB column equilibrated in MPA. Elution with 50 mM TEAA, 18% ACN, pH 7.0 (mobile phase B, MPB) was subsequently performed in 95 CV long linear gradient or steps at temperature and flow rate as described in the results section. For subsequent analytics, elution fractions were immediately buffer exchanged into ddH₂O, using Vivacon 500 by loading 500 μ L of sample onto the filter, centrifuging for 4 min at 4,000 \times g, washing three times with 450 μ L of ddH₂O, and concentrating to approximately 50 μ L. RNA concentration was determined using NanoDrop One (Thermo Fisher Scientific).

Before each chromatographic experiment, CIM SDVB monoliths, with the exception of 80 mL, were sanitized with at least 10 CV (column volume) of 50 mM TEAA and 75% ACN (contact time 15 min), followed by equilibration with MPA. To test a variation of sanitization procedure without ACN, CIMmultus SDVB 80 mL column was washed with ddH₂O in a 10 CV linear gradient, sanitized with 10 CV of 1 M NaOH (contact time 15 min), neutralized with 10 CV of 1 M ammonium acetate (contact time 15 min), followed by 10 CV of ddH₂O, and finally equilibrated with MPA in a 10 CV linear gradient (10 min contact time).

Small-scale chromatographic experiments on CIM SDVB spin column with 0.1 mL monolith (Sartorius BIA Separations, not commercially available) were performed using a MiniSpin centrifuge (Eppendorf) operated at 1,000 rpm for 8 min per cycle. For each experiment, 95 μ g of Oligo dT-prepurified mRNA sample was diluted 10-fold with MPA to final volume of 600 μ L and loaded onto equilibrated spin column. Elution with 600 μ L of 50 mM TEAA buffers containing 8.5%, 11.7%, and 18.0% ACN, pH 7.0, was subsequently performed. Elution fractions were immediately buffer exchanged into ddH₂O using Vivacon 500 as described above. RNA concentration was determined using NanoDrop One (Thermo Fisher Scientific). After each experiment, spin columns were washed with 500 μ L of ddH₂O, sanitized with 500 μ L of 0.5 M NaOH, neutralized with 500 μ L of 1 M ammonium acetate, washed again with 500 μ L of ddH₂O, and finally equilibrated with 2x 500 μ L of MPA.

Electrophoretic analyses

Buffer-exchanged SDVB elution fractions were evaluated for purity and integrity on capillary gel and agarose gel electrophoresis (AGE). Analyses on Fragment Analyzer (FA) 5200 (Agilent Technologies) were performed according to manufacturer's instructions for RNA kit (15 nt) and AGE was performed as previously described.⁴⁴ AGE was also used to semi-quantitatively determine the amount of

residual linear pDNA template in purified RNA samples as described previously.⁴⁴ For this experiment, 10 µg of RNA sample was first incubated with RNase A for 1 h at 37°C prior to analysis, which enabled visualization of residual pDNA template in RNA samples. RNA in-process samples were resolved on PAGE using native 6% Novex TBE Gels or denaturing 6% Novex TBE-Urea Gels with the XCell SureLock Mini-Cell (both Invitrogen) according to the manufacturer's instructions. For the native gel, the samples were diluted to 10 ng/µL, mixed 1:4 with Novex Hi-Density TBE Sample Buffer (5X) and loaded on the gel. Electrophoresis was performed at 230 V for 60 min. For the denaturing gel, samples were diluted to 10 ng/µL, mixed 1:1 with Novex TBE-Urea Sample Buffer (2X), denatured for 3 min at 75°C and snap-cooled on ice for 5 min prior to loading. GeneRuler 1 kb Plus DNA Ladder was used for sizing. Electrophoresis was performed at 180 V for 300 min. After electrophoretic separation, gels were stained in TBE solution (89 mM Tris, 89 mM boric acid, 2 mM EDTA) containing 1X SYBR Gold for 5 min and the nucleic acids were visualized on iBright FL 1500 (Thermo Fisher Scientific).

J2 dot blot

Aliquots of SDVB fractions were analyzed on J2 dot blot for dsRNA detection. Positively charged Biodyne pre-cut nylon membrane and western blotting filter paper were first wetted in ddH₂O and placed into the sealing gasket of Minifold I 96-well system (Whatman). One hundred to 500 µL of sample containing approximately 1 µg of RNA was pipetted into each well and loaded onto the membrane by vacuum. Strip fractions were loaded at 0.5 µg due to higher intensity of J2 signal. Magi2 dsRNA standard was used as a positive control (10 ng per dot). The Minifold was then disassembled, and the membrane was transferred to blocking buffer containing 5% (w/v) non-fat dried milk in 1x Tris-buffered saline with Tween 20 (TBS-T) for 15 min, followed by one wash with 1x TBS-T buffer for 1 min. For dsRNA detection, the membrane was incubated for 30 min in 1x TBS-T buffer containing 1% (w/v) non-fat dried milk, 5,000x diluted anti-dsRNA primary antibody J2 and 5,000x diluted secondary antibody Peroxidase AffiniPure Goat Anti-Mouse IgG (H + L). Finally, the membrane was washed (5 × 5 min) in 1x TBS-T buffer and chemiluminescent signal was visualized with WesternBright ECL on iBright FL1500 imaging system (Thermo Fisher Scientific).

LC analytics of residual pDNA template

CIMac pDNA analytical column (Sartorius BIA Separations) with 0.3-mL bed volume and average channel size of 1.4 µm was used to quantitate the amount residual pDNA template in RNA samples as published previously.³⁸ Briefly, 10 µg of RNA sample was first incubated with 20 ng of RNase A for 1 h at 37°C to digest RNA and enable visualization of >2 ng of residual linear pDNA. Samples were then diluted 10-fold in binding buffer and injected onto the column for separation of digested RNA fragments from residual pDNA template. The concentration of residual pDNA template in RNA samples was calculated from the calibration curve prepared with linear pDNA standard, by integrating peak area of the UV 260 nm signal.

Capping efficiency

Relative amount of 5' capped and uncapped RNA in IVT reaction was evaluated with a two-step enzymatic reaction based on Chiron and Jais,⁴⁵ coupled with HPLC determination of RNA concentration as described before.⁴⁶ First, 5'-triphosphate was removed from RNA sample by mixing 20 U of RNase Inhibitor, 1 µg of mRNA (RNA mass determined by CIMac PrimaS method), 10 U of RNA 5' Polyphosphatase, and RNA 5' Polyphosphatase Reaction Buffer in 20 µL total reaction volume. The mixture was incubated at 37°C for 60 min and then mixed with 0.5 U of Terminator 5'-Phosphate-Dependent Exonuclease and 20 U of RNase inhibitor in Terminator Reaction Buffer A to 40 µL final volume. This mixture was further incubated at 30°C for 30 min and finally quenched with 5 mM EDTA, pH 8.0 (final concentration). The concentration of undigested (capped) RNA and control RNA (non-processed RNA) were determined with CIMac PrimaS analytical method as described previously. Capping efficiency was calculated as a quotient of digested RNA and undigested control.

Oligo dT quantification of polyadenylated mRNA

Buffer-exchanged SDVB elution fractions were analyzed using a CIMac Oligo dT column (Sartorius BIA Separations) with 0.1 mL bed volume and an average channel size of 2 µm, to quantify polyadenylated mRNA as described before,⁴⁷ with the following modifications: mRNA samples were prepared for injection by a 10-fold dilution in MPA (50 mM Na-phosphate, 0.5 M NaCl, pH 7.4) and 1 µg was injected on the column. A step to MPB (50 mM Na-phosphate, pH 7.4) removed non-specifically bound RNA and a step to ddH₂O eluted polyadenylated mRNA. After each injection the column was washed with 0.5 M NaOH. Flow rate was 1 mL/min throughout the analysis. The peaks were integrated and the amount of bound (polyadenylated) mRNA and unbound (flow-through and wash) sequences was calculated as percentage of total peak area.

Cell culture

BHK-21 cells were cultured in Eagle's minimum essential medium and A549 cells in F-12K Nutrient Mixture-Kaighn's Modification medium. Media of both cell types were supplemented with 10% fetal calf serum. Peripheral blood mononuclear cells (PBMCs) were isolated from buffy coats obtained from the Transfusion Center of the University Medical Center of the Johannes Gutenberg University Mainz by Ficoll gradient and cultivated in RPMI medium containing 5% plasma-derived pooled human serum, 1% non-essential amino acids, and 1 mM sodium pyruvate. All cells were grown at 37°C in a humidified atmosphere equilibrated to 5% CO₂.

RNA transfection

For lipofection, 10,000 A549 cells, 5,000 BHK21, or 400,000 PBMCs were seeded in 100 µL medium per well into a Nunc MicroWell 96 Well plate and left to adhere. RNAs were prepared in RNase-free tubes and complexed with Lipofectamine MessengerMax in OptiMEM following the manufacturer's instructions. Per 100 ng RNA, RNA was diluted in 5 µL OptiMEM and mixed with 0.4 µL MessengerMax in 5 µL OptiMEM.

Firefly luciferase expression

At the desired time points post transfection, either 30 μ L Bright Glo reagent to access transgene expression or 50 μ L CellTiter Glo to analyze cell viability via ATP concentration was added to the cells and incubated for 3 min at room temperature. After incubation, the emitted luciferase signal was measured with an integration time of 1,000 ms using a Spark multimode microplate reader.

Flow cytometry

GFP expression was quantified by flow cytometry. Therefore, cells were harvested, washed with PBS, and fixed with PBS containing 4% formaldehyde. GFP expression was detected using a FACS Canto II flow cytometer (BD Biosciences) and analyzed using the FACSDiva or FloJo v10 software (both BD Bioscience).

ELISA

To detect secreted human IFN β , luciferase-based sandwich ELISA kit (Invivogen) was used according to the manufacturer's instructions. Supernatants of transfected cells were collected and stored at -80°C until usage. Luminescence was detected with a Spark multimode microplate reader.

Statistical analysis

Statistical analysis was performed with GraphPad Prism 10. Statistical differences between two groups were calculated using two-sided unpaired t tests. p values lower than 0.05 were considered as significant and classified into $*p < 0.05$; $**p < 0.01$; $***p < 0.001$; $****p < 0.0001$.

DATA AVAILABILITY

The data that support the findings of this study are available from the corresponding author upon reasonable request.

ACKNOWLEDGMENTS

The authors would like to thank Tomas Kostelec, Urh Černigoj, and Jasmina Puc for helpful discussions during preparation of the manuscript. In addition, Klemen Božič, Tina Vodopivec Seravalli, Neža Trampuž, Nana Ries, and Aleksandra Vončina are acknowledged for experimental and analytical support during the studies. Božo Žgavc and Jana Vidič are acknowledged for providing prototype CIM SDVB spin columns used in the study.

Yscript research project is also gratefully acknowledged for funding. Yscript has received funding from the European Innovation Council (EIC) under grant agreement no 101047214. The EIC receives support from the European Union's Horizon Europe research and innovation program. The content provided in this manuscript reflects the authors' views only.

Dedicated to the memory of Milena Miklavec Krušič (1959–2024).

AUTHOR CONTRIBUTIONS

A.K.: conceptualization, experimental design, data analysis, manuscript writing. N.M.: conceptualization, experimental design, data analysis, manuscript writing, and editing. M.L.: experimental design, data analysis. E.N.: conceptualization, experimental design, data analysis, manuscript writing. M.P.: conceptualization, experimental design, data analysis, manuscript writing, and editing. U.S.: conceptualization, manuscript editing. P.M.: experimental design, data analysis. A.Š.: conceptualization, manuscript editing. R.S.: conceptualization, experimental design, data analysis, manuscript writing, and editing.

DECLARATION OF INTERESTS

A.K., N.M., M.L., P.M., A.Š., and R.S. are employees of Sartorius BIA Separations, d.o.o., which provided columns and chromatography systems used for this work.

SUPPLEMENTAL INFORMATION

Supplemental information can be found online at <https://doi.org/10.1016/j.omtn.2025.102491>.

REFERENCES

- Sahin, U., Karikó, K., and Türeci, Ö. (2014). mRNA-based therapeutics — developing a new class of drugs. *Nat. Rev. Drug Discov.* 13, 759–780. <https://doi.org/10.1038/nrd4278>.
- Kozlova, N.V., Pichon, C., and Rahmouni, A.R. (2020). mRNA with Mammalian Codon Bias Accumulates in Yeast Mutants with Constitutive Stress Granules. *Int. J. Mol. Sci.* 21, 1234. <https://doi.org/10.3390/ijms21041234>.
- Curry, E., Muir, G., Qu, J., Kis, Z., Hulley, M., and Brown, A. (2024). Engineering an Escherichia coli based in vivo mRNA manufacturing platform. *Biotechnology and Bioengineering n/a. Biotechnol. Bioeng.* 121, 1912–1926. <https://doi.org/10.1002/bit.28684>.
- Rosa, S.S., Prazeres, D.M.F., Azevedo, A.M., and Marques, M.P.C. (2021). mRNA vaccines manufacturing: Challenges and bottlenecks. *Vaccine* 39, 2190–2200. <https://doi.org/10.1016/j.vaccine.2021.03.038>.
- Lenk, R., Kleindienst, W., Szabó, G.T., Baiersdörfer, M., Boros, G., Keller, J.M., Mahiny, A.J., and Vlatkovic, I. (2024). Understanding the impact of in vitro transcription byproducts and contaminants. *Front. Mol. Biosci.* 11, 1426129. <https://doi.org/10.3389/fmolb.2024.1426129>.
- García, M.A., Gil, J., Ventoso, I., Guerra, S., Domingo, E., Rivas, C., and Esteban, M. (2006). Impact of protein kinase PKR in cell biology: from antiviral to antiproliferative action. *Microbiol. Mol. Biol. Rev.* 70, 1032–1060. <https://doi.org/10.1128/MMBR.00027-06>.
- Sonenberg, N., and Hinnebusch, A.G. (2009). Regulation of translation initiation in eukaryotes: mechanisms and biological targets. *Cell* 136, 731–745. <https://doi.org/10.1016/j.cell.2009.01.042>.
- Romanovskaya, A., Sarin, L.P., Bamford, D.H., and Poranen, M.M. (2013). High-throughput purification of double-stranded RNA molecules using convective interaction media monolithic anion exchange columns. *J. Chromatogr. A* 1278, 54–60. <https://doi.org/10.1016/j.chroma.2012.12.050>.
- Kim, I., McKenna, S.A., Viani Puglisi, E., and Puglisi, J.D. (2007). Rapid purification of RNAs using fast performance liquid chromatography (FPLC). *RNA* 13, 289–294. <https://doi.org/10.1261/rna.342607>.
- Dewar, E.A., Guterstam, P., Holland, D., Lindman, S., Lundbäck, P., Brito Dos Santos, S., Wang, S.C., and Swartz, A.R. (2024). Improved mRNA affinity chromatography binding capacity and throughput using an oligo-dT immobilized electrospun polymer nanofiber adsorbent. *J. Chromatogr. A* 1717, 464670. <https://doi.org/10.1016/j.chroma.2024.464670>.
- Easton, L.E., Shibata, Y., and Lukavsky, P.J. (2010). Rapid, nondenaturing RNA purification using weak anion-exchange fast performance liquid chromatography. *RNA* 16, 647–653. <https://doi.org/10.1261/rna.1862210>.
- Summer, H., Grämer, R., and Dröge, P. (2009). Denaturing Urea Polyacrylamide Gel Electrophoresis (Urea PAGE). *J. Vis. Exp.* 1485. <https://doi.org/10.3791/1485>.
- Masuda, N., Ohnishi, T., Kawamoto, S., Monden, M., and Okubo, K. (1999). Analysis of chemical modification of RNA from formalin-fixed samples and optimization of molecular biology applications for such samples. *Nucleic Acids Res.* 27, 4436–4443.
- Megušar, P., Miklavčič, R., Korenč, M., Ličen, J., Vodopivec, T., Černigoj, U., Štrancar, A., and Sekirnik, R. (2023). Scalable multimodal weak anion exchange chromatographic purification for stable mRNA drug substance. *Electrophoresis* 44, 1978–1988. <https://doi.org/10.1002/elps.202300106>.
- Miklavčič, R., Megušar, P., Kodermac, Š.M., Bakalar, B., Dolenc, D., Sekirnik, R., Štrancar, A., and Černigoj, U. (2023). High Recovery Chromatographic Purification of mRNA at Room Temperature and Neutral pH. *Int. J. Mol. Sci.* 24, 14267. <https://doi.org/10.3390/ijms241814267>.

16. Baierdörfer, M., Boros, G., Muramatsu, H., Mahiny, A., Vlatkovic, I., Sahin, U., and Karikó, K. (2019). A Facile Method for the Removal of dsRNA Contaminant from In Vitro-Transcribed mRNA. *Mol. Ther. Nucleic Acids* 15, 26–35. <https://doi.org/10.1016/j.omtn.2019.02.018>.
17. Nicholson, A.W. (2014). Ribonuclease III mechanisms of double-stranded RNA cleavage. *Wiley Interdiscip. Rev. RNA* 5, 31–48. <https://doi.org/10.1002/wrna.1195>.
18. Foster, J.B., Choudhari, N., Perazzelli, J., Storm, J., Hofmann, T.J., Jain, P., Storm, P.B., Pardi, N., Weissman, D., Waanders, A.J., et al. (2019). Purification of mRNA Encoding Chimeric Antigen Receptor Is Critical for Generation of a Robust T-Cell Response. *Hum. Gene Ther.* 30, 168–178. <https://doi.org/10.1089/hum.2018.145>.
19. Karikó, K., Muramatsu, H., Ludwig, J., and Weissman, D. (2011). Generating the optimal mRNA for therapy: HPLC purification eliminates immune activation and improves translation of nucleoside-modified, protein-encoding mRNA. *Nucleic Acids Res.* 39, e142. <https://doi.org/10.1093/nar/gkr695>.
20. Nwokeoji, A.O., Kung, A.-W., Kilby, P.M., Portwood, D.E., and Dickman, M.J. (2017). Purification and characterisation of dsRNA using ion pair reverse phase chromatography and mass spectrometry. *J. Chromatogr. A* 1484, 14–25. <https://doi.org/10.1016/j.chroma.2016.12.062>.
21. Weissman, D., Pardi, N., Muramatsu, H., and Karikó, K. (2013). HPLC Purification of In Vitro Transcribed Long RNA. In *Synthetic Messenger RNA and Cell Metabolism Modulation: Methods and Protocols*, P.M. Rabinovich, ed. (Humana Press), pp. 43–54. https://doi.org/10.1007/978-1-62703-260-5_3.
22. Azarani, A., and Hecker, K.H. (2001). RNA analysis by ion-pair reversed-phase high performance liquid chromatography. *Nucleic Acids Res.* 29, e7.
23. Dickman, M.J., and Hornby, D.P. (2006). Enrichment and analysis of RNA centered on ion pair reverse phase methodology. *RNA* 12, 691–696. <https://doi.org/10.1261/rna.2278606>.
24. Duncan, J.K., Chen, A.J., and Siebert, C.J. (1987). Performance evaluation of non-porous versus porous ion-exchange packings in the separation of proteins by high-performance liquid chromatography. *J. Chromatogr. A* 397, 3–12. [https://doi.org/10.1016/S0021-9673\(01\)84985-2](https://doi.org/10.1016/S0021-9673(01)84985-2).
25. Martin, M., and Guiochon, G. (2005). Effects of high pressure in liquid chromatography. *J. Chromatogr. A* 1090, 16–38. <https://doi.org/10.1016/j.chroma.2005.06.005>.
26. Mencin, N., Štepec, D., Margon, A., Vidič, J., Dolenc, D., Simčič, T., Rotar, S., Sekirnik, R., Štrancar, A., and Černigoj, U. (2023). Development and scale-up of oligo-dT monolithic chromatographic column for mRNA capture through understanding of base-pairing interactions. *Separ. Purif. Technol.* 304, 122320. <https://doi.org/10.1016/j.seppur.2022.122320>.
27. Eriksson, S., Glad, G., Pernemalm, P.-Å., and Westman, E. (1986). Separation of DNA restriction fragments by ion-pair chromatography. *J. Chromatogr. A* 359, 265–274. [https://doi.org/10.1016/0021-9673\(86\)80080-2](https://doi.org/10.1016/0021-9673(86)80080-2).
28. Gagnon, P. (2020). *Purification of Nucleic Acids (BIA Separations)*.
29. Budihna, A.F., Celjar, A.M., Lebar, S., Livk, A.G., and Štrancar, A. (2023). mRNA fragmentation and quality assessment using ion pair reverse-phase analytics. *Cell and Gene Therapy Insights* 9, 1231–1247. <https://doi.org/10.18609/cgti.2023.161>.
30. Otsuki, K., Noro, K., Yamamoto, H., and Tsubokura, M. (1979). Studies on avian infectious bronchitis virus (IBV). II. Propagation of IBV in several cultured cells. *Arch. Virol.* 60, 115–122. <https://doi.org/10.1007/BF01348027>.
31. Marchese, A.M., Chiale, C., Moshkani, S., and Robek, M.D. (2020). Mechanisms of Innate Immune Activation by a Hybrid Alphavirus-Rhabdovirus Vaccine Platform. *J. Interferon Cytokine Res.* 40, 92–105. <https://doi.org/10.1089/jir.2019.0123>.
32. Fordyce, S.L., Kampmann, M.-L., van Doorn, N.L., and Gilbert, M.T.P. (2013). Long-term RNA persistence in postmortem contexts. *Investig. Genet.* 4, 7. <https://doi.org/10.1186/2041-2223-4-7>.
33. Milligan, J.F., Groebe, D.R., Witherell, G.W., and Uhlenbeck, O.C. (1987). Oligoribonucleotide synthesis using T7 RNA polymerase and synthetic DNA templates. *Nucleic Acids Res.* 15, 8783–8798.
34. Arnaud-Barbe, N., Cheynet-Sauvion, V., Oriol, G., Mandrand, B., and Mallet, F. (1998). Transcription of RNA templates by T7 RNA polymerase. *Nucleic Acids Res.* 26, 3550–3554. <https://doi.org/10.1093/nar/26.15.3550>.
35. Daube, S.S., and von Hippel, P.H. (1994). RNA displacement pathways during transcription from synthetic RNA-DNA bubble duplexes. *Biochemistry* 33, 340–347. <https://doi.org/10.1021/bi00167a044>.
36. Nacheva, G.A., and Berzal-Herranz, A. (2003). Preventing undesired RNA-primed RNA extension catalyzed by T7 RNA polymerase. *Eur. J. Biochem.* 270, 1458–1465. <https://doi.org/10.1046/j.1432-1033.2003.03510.x>.
37. Triana-Alonso, F.J., Dabrowski, M., Wadzack, J., and Nierhaus, K.H. (1995). Self-coded 3'-extension of run-off transcripts produces aberrant products during in vitro transcription with T7 RNA polymerase. *J. Biol. Chem.* 270, 6298–6307. <https://doi.org/10.1074/jbc.270.11.6298>.
38. Leban, M., Vodopivec Seravalli, T., Hauer, M., Böhm, E., Mencin, N., Potušek, S., Thompson, A., Trontelj, J., Štrancar, A., and Sekirnik, R. (2024). Determination of linearized pDNA template in mRNA production process using HPLC. *Anal. Bioanal. Chem.* 416, 2389–2398. <https://doi.org/10.1007/s00216-024-05204-0>.
39. Nelson, J., Sorensen, E.W., Mintri, S., Rabideau, A.E., Zheng, W., Besin, G., Khatwani, N., Su, S.V., Miracco, E.J., Issa, W.J., et al. (2020). Impact of mRNA chemistry and manufacturing process on innate immune activation. *Sci. Adv.* 6, eaaz6893. <https://doi.org/10.1126/sciadv.aaz6893>.
40. Vogel, A.B., Lambert, L., Kinnear, E., Busse, D., Erbar, S., Reuter, K.C., Wicke, L., Perkovic, M., Beissert, T., Haas, H., et al. (2018). Self-Amplifying RNA Vaccines Give Equivalent Protection against Influenza to mRNA Vaccines but at Much Lower Doses. *Mol. Ther.* 26, 446–455. <https://doi.org/10.1016/j.ymthe.2017.11.017>.
41. McGee, J.E., Kirsch, J.R., Kenney, D., Chavez, E., Shih, T.-Y., Douam, F., Wong, W.W., and Grinstaff, M.W. (2023). Complete substitution with modified nucleotides suppresses the early interferon response and increases the potency of self-amplifying RNA. Preprint at bioRxiv. <https://doi.org/10.1101/2023.09.15.557994>.
42. Komori, M., Morey, A.L., Quiñones-Molina, A.A., Fofana, J., Romero, L., Peters, E., Matsuda, K., Gummuluru, S., Smith, J.F., Akahata, W., et al. (2023). Incorporation of 5 methylcytidine alleviates innate immune response to self-amplifying RNA vaccine. Preprint at bioRxiv. <https://doi.org/10.1101/2023.11.01.565056>.
43. Korenč, M., Mencin, N., Puc, J., Skok, J., Nemec, K.Š., Celjar, A.M., Gagnon, P., Štrancar, A., and Sekirnik, R. (2021). Chromatographic purification with CIMmultus™ Oligo dT increases mRNA stability. *Cell and Gene Therapy Insights* 7, 1207–1216. <https://doi.org/10.18609/cgti.2021.161>.
44. Skok, J., Megušar, P., Vodopivec, T., Pregelj, D., Mencin, N., Korenč, M., Krušič, A., Celjar, A.M., Pavlin, N., Krušič, J., et al. (2022). Gram-Scale mRNA Production Using a 250-mL Single-Use Bioreactor. *Chem. Ing. Tech.* 94, 1928–1935. <https://doi.org/10.1002/cite.202200133>.
45. Chiron, S., and Jais, P.H. (2017). Non-radioactive monitoring assay for capping of messenger RNA. *Translational Genetics and Genomics* 1, 46–49.
46. Pregelj, D., Skok, J., Vodopivec, T., Mencin, N., Krušič, A., Ličen, J., Nemec, K.Š., Štrancar, A., and Sekirnik, R. (2023). Increasing yield of in vitro transcription reaction with at-line high pressure liquid chromatography monitoring. *Biotechnol. Bioeng.* 120, 737–747. <https://doi.org/10.1002/bit.28299>.
47. Dayeh, D.M., Cika, J., Moon, Y., Henderson, S., Di Grandi, D., Fu, Y., Muthusamy, K., Palackal, N., Ihnat, P.M., and Pyles, E.A. (2024). Comprehensive chromatographic assessment of forced degraded in vitro transcribed mRNA. *J. Chromatogr. A* 1722, 464885. <https://doi.org/10.1016/j.chroma.2024.464885>.